



Spatially resolved local intracellular chemical sensing using magnetic particles

S. Shekhar^a, A. Klaver^a, C.G. Figdor^b, V. Subramaniam^a, J.S. Kanger^{a,*}

^a Nanobiophysics, MIRA Institute for Biomedical Technology and Technical Medicine, University of Twente, PO Box 217, 7500 AE, Enschede, The Netherlands

^b Department of Tumor Immunology, Nijmegen Center for Molecular Life Sciences, Radboud University, P.O. Box 9101, 6500 HB, Nijmegen, The Netherlands

ARTICLE INFO

Article history:

Received 2 March 2010

Received in revised form 27 April 2010

Accepted 3 May 2010

Available online 9 May 2010

Keywords:

Magnetic tweezers

Magnetic particles

Spatially resolved

Chemical sensing

Phagocytosis

ABSTRACT

In this paper we present a new approach that allows spatially resolved local intracellular chemical sensing using a hybrid magnetic chemical sensor which can be actively manipulated inside a cell. This approach allows the sensor to be maneuvered to specific locations in the cell without the need of additional specific biochemical targeting. The approach causes minimal interference within the cell as only a single particle is needed to measure the chemical property at different sites inside the cell. In addition high differential accuracy in measuring the chemical property can be achieved as the same sensor is used to measure at different locations, and therefore the measurements are not affected by sensor-to-sensor variations. To this end we couple a chemical sensor to a magnetic particle and use magnetic tweezers to position and move the sensor inside the living cell in order to measure local chemical properties at different sites inside the cell. We illustrate the potential of this approach by moving a phagocytosed hybrid pH-sensing magnetic particle through a cell while simultaneously measuring the pH of the phagosome.

© 2010 Elsevier B.V. All rights reserved.

1. Introduction

The living cell is a complex entity in which a vast number of micro-environments and a myriad of cellular organelles co-exist. The micro-environments are often separated from each other by membrane boundaries of cellular organelles. Intracellular processes strongly rely on the precise spatial and temporal distribution of chemical metabolites and proteins that traffic between intracellular organelles [1–4]. It is therefore important to visualize and understand the spatially resolved intracellular distribution of specific chemical species. In order to study chemical distributions in cells, it is essential to devise biophysical tools that will allow spatially resolved measurement of individual chemical species with high specificity and sensitivity.

Fluorescence microscopy has been the technique of choice for quantitative intracellular measurements of chemical molecules. Free fluorescent dyes can be delivered to cells for intracellular sensing. Many different dyes are available whose fluorescence intensities specifically depend on the concentration of specific analytes (e.g. Ca^{2+} , pH, O_2). Although this fluorescent sensing prin-

ciple has been successfully applied to cells, the free nature of the dyes leads to some major drawbacks. Free dyes can be selectively sequestered in different organelles, or bind non-specifically to proteins and other cell components and are also difficult to target to specific locations inside the cell [5]. For these reasons, this principle has been further refined by coupling the dyes to micrometer and nanometer-sized particles and using these particles as intracellular sensors [5]. This approach allows selective delivery of the sensor for spatially resolved sensing. A very interesting example of this approach is the development of polyacrylamide nanoparticles, called PEBBLE sensors. PEBBLE sensors have been used for ratio-metric sensing of ions like H^+ , Ca^{2+} , Mg^{2+} , Zn^{2+} , Cu^{+2+} and Fe^{3+} [6]. PEBBLE phosphate sensors have been developed by embedding fluorescent reporter proteins (FLIPPi) in polyacrylamide nanoparticles [7]. Near-infrared phosphorescent probes to sense molecular oxygen [8], sensors for reactive oxygen species like singlet oxygen [9], hydroxyl radicals [10] and hydrogen peroxide [11] and ratio-metric glucose sensors [12] have also been developed. In addition to sensing specific chemical analytes, nanoparticle-based sensors have also been developed for studying cellular processes like apoptosis [13] and lipid peroxidation [14].

Particle-based sensors used so far have shown great potential for intracellular use and have solved most of the limitations associated with the use of free fluorescent dyes. However a few issues still remain. In particular, specific targeting to organelles is possible, but full control on their position within the cell has not yet been possible. In addition, a large number of particles are needed to carry out cell-wide experiments that may interfere with normal cell function. In order to address these issues we here propose the

Abbreviations: MT, magnetic tweezers; M270-FL-TR, dynal M270 beads labeled with Fluorescein and Texas Red dyes; M270-OG-TR, dynal M270 beads labeled with Oregon Green and Texas Red dyes; M270-SNARF, dynal M270 beads labeled with SNARF-4f dye.

* Corresponding author. Tel.: +31 534893726; fax: +31 534891105.

E-mail addresses: j.s.kanger@tnw.utwente.nl, j.s.kanger@utwente.nl (J.S. Kanger).

use of magnetic particle-based sensors. Magnetic tweezers (MT) have proven to be a versatile approach to move magnetic particles inside living cells [15,16]. The use of magnetic tweezers relies on the use of magnetic particles which can in turn be coupled to chemical sensing molecules. The magnetic content of the particles allows directed movement of the sensor within the living cell, controlled by externally applied magnetic fields. We believe this approach offers specific advantages over existing methods. (i) The sensor can be maneuvered to specific locations in the cell without the need of additional specific biochemical targeting. (ii) Minimized interference of the sensor with the cell as only a single particle is needed to measure the chemical property at different sites inside the cell. (iii) High differential accuracy as the same sensor is used to measure at different locations, and the measurements are not affected by sensor-to-sensor variations.

A limited number of examples on the coupling of chemical sensing dyes to magnetic particles have been reported. Roberts et al. loaded hybrid particles, MagMOONS, with Snarf-1f dye [17], Anker et al. used magnetically controlled sensor swarms to measure pH using PEBBLES with additional ferrite content [18], and Liu et al. synthesized magnetic nanoparticles coupled with Fluorescein. However, the particles used all have a low magnetic content and as such their potential for use in intracellular MT manipulation experiments are very limited. To our knowledge, only one study has so far used the magnetic nature of the fluorescent sensors for movement, relying on magnetically controlled sensor swarms to measure pH using nanoparticles conjugated with a pH-sensitive dye (PEBBLES) [18].

In this paper we demonstrate a new approach for spatially resolved intracellular chemical sensing. We develop a magnetic particle-based pH sensor and demonstrate a proof-of-principle of the proposed approach by measuring intracellular pH while simultaneously moving the sensor through the cell. Very interestingly, the results obtained demonstrate that this approach can also be used to actively interfere with specific cellular processes.

As an example of a proof-of-concept, we have chosen to utilize the process of phagocytosis. During this process the magnetic particle is internalized by the cells in a so-called phagosome. As a result of fusion of the phagosome with acidic cellular vesicles, the pH of the phagosome drops from 6.8 to ~4.5. This change in pH allows us to test the function of the magnetic pH sensor. In addition, an external force can be applied on the phagosome using the MT. The resulting displacement of the phagosome/magnetic particle sensor within the cell can be followed using white light microscopy.

2. Materials and methods

2.1. Materials

Amino-terminated Dynabeads M270 (diameter 2.7 μm , 20% ferrite content resulting in a magnetic moment of $\sim 150 \text{ fA m}^2$) were obtained from Dynal (Oslo, Norway). Sodium bicarbonate (NaHCO_3) was obtained from Merck (Darmstadt, Germany). Fluorescein, Oregon Green 488, and Texas Red with a succinimidyl ester (SE) linker group and Snarf-4f with a carboxylic linker group were obtained from Invitrogen – Molecular Probes Inc. (Eugene, OR, USA). 2-(N-morpholino) ethanesulfonic (MES) and 1-ethyl-3-(3-dimethylaminopropyl) carbodiimide hydrochloride (EDAC) were obtained from Sigma–Aldrich (Steinheim, Germany). Citric acid ($\text{C}_6\text{H}_8\text{O}_7$) and disodium hydrogen phosphate (Na_2HPO_4) used for the pH buffer solutions were acquired from BDH laboratory reagents (Karlsruhe, Germany) and Merck, respectively. Lab-tek chambered coverglass ($\sim 0.15\text{-mm}$ thick borosilicate) was obtained from Nalge Nunc International (Rochester, NY, USA). RPMI cell medium was purchased from Sigma–Aldrich, while the fetal bovine

serum, HEPES, l-glutamine and antibiotic–antimycotic were from Invitrogen – Molecular Probes Inc.

2.2. Preparation of pH buffers

0.1 M citric acid was mixed together with 0.2 M disodium hydrogen phosphate to obtain pH buffers from pH 3 to 8 as described by Dawson et al. [19].

2.3. Functionalization of magnetic, pH-sensing particles

Three different pH-sensing magnetic particles were prepared.

2.3.1. Dynal M270 with Fluorescein and Texas Red (abbreviated as M270-FL-TR)

The synthesis of M270-FL-TR is similar to the procedure published by Ji et al. for the synthesis of pH-sensing polystyrene particles [20]. SE functionalized Fluorescein was covalently coupled to amino-terminated M270-particles. Stock amino-terminated M270-particles (20 μl , 30 mg ml^{-1}) were diluted in sodium bicarbonate buffer (0.5 ml 0.1 M). Next, 0.5 ml of 900 μM Fluorescein SE dissolved in sodium bicarbonate buffer was added to the particle solution. Next, Texas Red-X SE dissolved in sodium bicarbonate buffer (0.5 ml of 600 μM) was added. This solution was placed on a tube-rotator overnight at 4 °C in the dark. Finally, the particles were washed six times using magnetic separation to remove excess dye.

2.3.2. Dynal M270 with Oregon Green and Texas Red (abbreviated as M270-OG-TR)

The same procedure was used as for the M270-FL-TR particles but instead of Fluorescein, 0.5 ml of 900 μM Oregon Green was used.

2.3.3. Dynal M270 with SNARF-4F (abbreviated as M270-SNARF)

Stock M270-particle solution (20 μl , 30 mg/ml) was suspended in 2-(N-morpholino) ethanesulfonic (MES) pH 6.15 Goods buffer (0.5 ml). 1-Ethyl-3-(3-dimethylaminopropyl) carbodiimide hydrochloride (EDAC, 50 mg) was dissolved into MES buffer (0.5 ml), added to the particle solution and incubated for 5 min. Then a Snarf-4f solution in MES buffer (0.5 ml, 200 μM) was added to the solution and incubated for 2 h at 4 °C in the dark, while mixing continuously. Finally, the particles were washed six times using magnetic separation to remove excess dye.

2.4. Fluorescence spectroscopy

The excitation spectra of M270-FL-TR and M270-OG-TR particles were measured using a fluorescence spectrophotometer (Cary Eclipse – Varian, Palo Alto, US). Oregon Green and Fluorescein were excited at 488 nm and the emission was measured from 500 to 600 nm with a step size of $\sim 1 \text{ nm}$ and a bandwidth of 10 nm. For Texas Red, an excitation of 543 nm was used and the emission was collected from 600 to 650 nm. Fluorescence spectra of M270-SNARF were measured using a Safire2 plate reader from Tecan (Grödig, Austria). The particles were excited at 543 nm, and the emission was measured from 565 to 750 nm. The nominal slit width was chosen such to have a spectral bandwidth of 10 nm for both excitation and emission.

2.5. Confocal microscope imaging

A Carl Zeiss (Göttingen, Germany) LSM 510 confocal laser scanning microscope (CLSM) was used to image individual particles. Single-track imaging was used to observe individual M270-SNARF

Table 1

Fluorescence excitation wavelength, λ , and detection filters used in the confocal microscope and wavelength ranges used to determine fluorescence peak area to determine fluorescence ratio R from spectroscopy results.

	λ_1 (nm)	Channel 1 (nm)	λ_2 (nm)	Channel 2 (nm)	R
M270-FL-TR	488	500–550	543	565–615	Ch. 1/Ch. 2
M270-OG-TR	488	500–550	543	565–615	Ch. 1/Ch. 2
M270-SNARF	543	565–615	543	650–750	Ch. 1/Ch. 2

particles. Multi-track imaging was used to image individual M270-FL-TR and M270-OG-TR particles. The observed channels with their corresponding excitation wavelengths and detector filters are given in Table 1 for all particles used.

2.6. Ratiometric analysis of fluorescence spectra

From each fluorescence spectrum a fluorescence intensity ratio, R , was calculated. Table 1 shows the wavelength ranges used to determine the fluorescence peak areas in the measured fluorescence spectra and the subsequent ratio calculation. To compare the ratios obtained by fluorescence spectroscopy and confocal imaging, the ratio found at pH 7 was indexed to 1 by normalizing all measured ratios by the ratio obtained at pH 7.

2.7. Ratiometric analysis of confocal images

The fluorescence emission ratios, R , of individual particles in the confocal images were obtained using a custom script written in ImageJ (National Institute of Health). First, the position of the particles in the images was determined by applying an appropriate threshold and subsequent particle detection. In case of M270-FL-TR and M270-OG-TR particles, channel 2 related to the pH-insensitive dye was used for particle detection, while channel 1 was used in case of M270-SNARF particles. Only spherical particles with an expected size of $\sim 2.7 \mu\text{m}$ were chosen for further analysis. In this way, particle aggregates and/or other impurities were ignored. The integrated fluorescence intensity of each detected particle was calculated for both channels and the fluorescence ratio R was determined by dividing the integrated intensity of the particle in channel 1 by the integrated intensity of channel 2. Finally, the average fluorescence ratio and the standard deviation were calculated.

2.8. Phagocytosis assay

RAW 264.7 cells were incubated overnight in a chambered cover glass at 37°C and 5% CO_2 atmosphere. The chamber was then placed on the CLSM microscope stage that was maintained at 37°C . The cell culture medium was replaced with RPMI medium without FCS and l-glutamine, but with 30 mM HEPES in order to maintain the appropriate medium pH. In addition, pH-sensing magnetic particles (approx. 4×10^5 particles/ml of medium) were added. Particle internalization and subsequent acidification of the phagocytosed particles was recorded by time-lapse imaging (both fluorescent and transmission images were taken every 45 s during 40 min).

2.9. Particle tracking

To measure the displacement of the particles inside cells the position of the particle was determined in each measured frame using a custom-written Labview application. The accuracy of this method is $\sim 8 \text{ nm}$ in both directions of the measuring plane. To achieve this accuracy the particle has to be slightly out of focus such that the observed diffraction pattern is clearly distinct from other cellular organelles or structures.

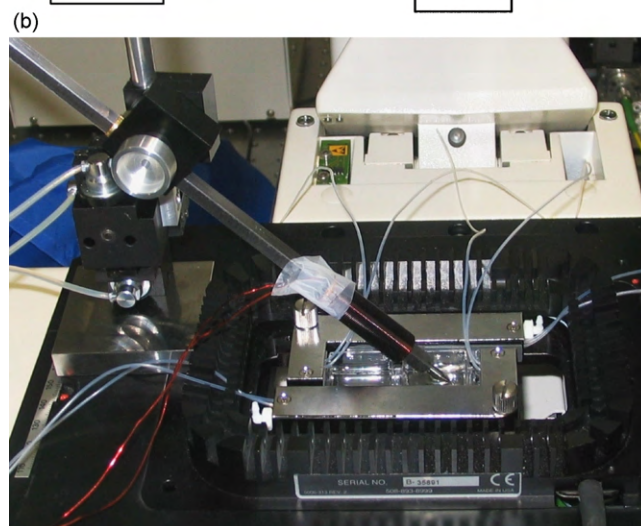
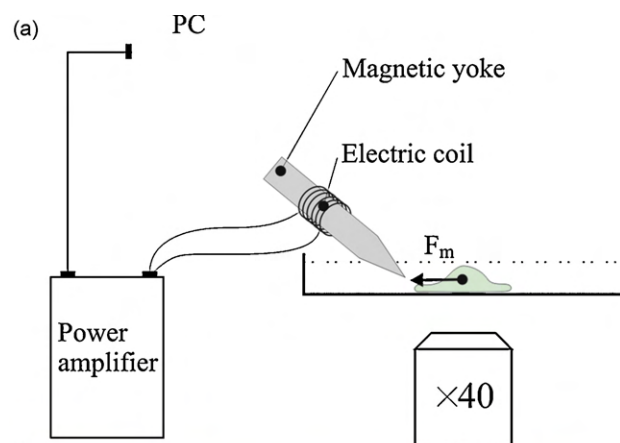


Fig. 1. (a) Schematic representation of the magnetic tweezers set-up. The current in the coil is computer-controlled. F_m denotes the magnetic force exerted on the particle by the magnetic tweezers. The magnetic tweezers set-up is assembled on a Zeiss LSM 510 confocal laser scanning microscope. (b) Photograph of the MT set-up. It consists of an iron rod with an electric coil wrapped around it. The iron rod is positioned using a micromanipulator. The MT is placed on a confocal fluorescence microscope.

2.10. Magnetic tweezers

A single pole magnetic tweezers consisting of an iron rod with a sharp tip (feature size $100 \mu\text{m}$) was used. Magnetic fields are generated using an electrical coil wrapped around the rod (250 ampere-turns). The magnetic tip was positioned accurately using a xyz micromanipulator. The magnetic tweezers were integrated with the CLSM. Using viscosity-drag calibrations, the maximum magnetic force that can be exerted on a M270 particle was determined to be $\sim 1 \text{ nN}$ at a distance of $10 \mu\text{m}$ from the pole tip to $\sim 0.1 \text{ nN}$ at a distance of $100 \mu\text{m}$ from the pole tip. A schematic of the set-up is shown in Fig. 1a and a photograph of the MT set-up placed on a confocal fluorescence microscope stage is shown in Fig. 1b.

3. Results

The data obtained with the M270-FL-TR and the M270-OG-TR particles are comparable to the data obtained for M270-SNARF particles. We limit the data presented here to M270-SNARF particles because these particles rely on a single dye, which simplifies the assay. Data from the M270-FL-TR and the M270-OG-TR particles can be found in the supplementary information. The fluorescence emission spectra of M270-SNARF particles in various pH buffers

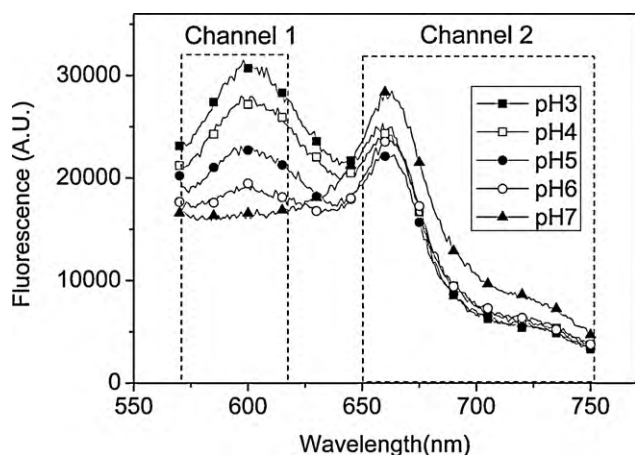


Fig. 2. Fluorescence emission spectra of M270-SNARF particles in various pH buffer solutions. The wavelength ranges of the two measuring channels are denoted by the two dotted boxes.

ranging from pH 3 to 7 are shown in Fig. 2. The ratio of the intensities of channel 1 and channel 2 is a measure of the pH. The total intensity for the two channels was calculated by integrating the intensity between specific wavelength ranges (see Table 1 and Fig. 2).

CLSM images of fluorescence emission for channel 1 and channel 2 were acquired by using appropriate band-pass filters. The ranges of wavelengths of the band-pass filters have been summarized in Table 1. We verified that the shape and size uniformity of particles was maintained after the dye functionalization procedure (Fig. 3). The M270-SNARF particles remained mono-disperse in solution. Uniformity of size and shape prevents differences in uptake and trafficking of the particles due to structural differences [21,22]. These particles show significant signal in both channels in the pH range 3–7. Variations in the amount of dye per particle were evaluated by comparing the fluorescence intensities for different particles. Particle-to-particle variation in intensity is

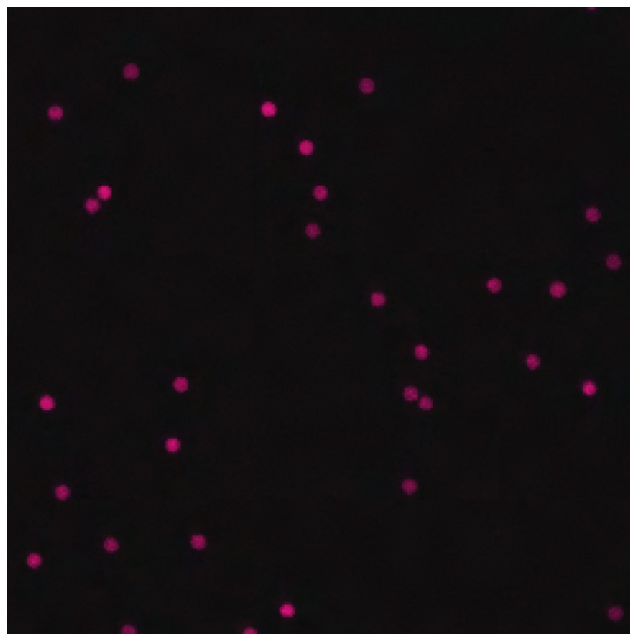


Fig. 3. Confocal fluorescence microscopy image of M270-SNARF particles on a glass substrate recorded for channel 2 (660 nm peak) at pH 5. The image shows that the magnetic particles remain mono-dispersed and do not show any appreciable change in their size and structure as a result of their chemical functionalization.

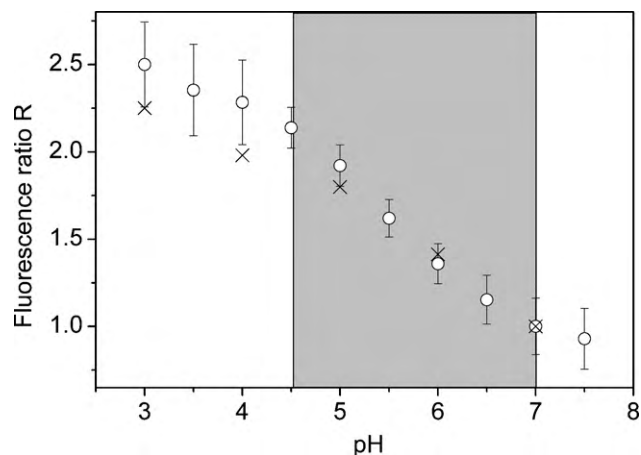


Fig. 4. Fluorescence ratio R of M270-SNARF particles in different pH buffers as determined from fluorescence spectroscopy (crosses) and CLSM (open circles). The grayed area indicates the relevant physiological pH range for phagocytosis (pH 4.5–6.8).

typically within 20% for both the channels. The variations in fluorescence ratios (as a measure of pH) are found to be much smaller as will be discussed later.

Fig. 4 shows the fluorescence ratio R as function of the pH as calculated from both the fluorescence spectroscopy data (for an ensemble of particles) and the CLSM data (of individual particles). The results from both methods are in good agreement. The dependence of the observed fluorescence ratio on the pH are similar to those found in literature for free dye [23,24].

Fig. 5 shows the standard deviation σ_{pH} in the measured pH as a function of the pH derived from the expression:

$$\sigma_{pH}(pH) = \frac{\sigma_R(pH)}{(dR/dpH)_{pH}} \quad (1)$$

where σ_R is the standard deviation in the ratio R obtained from the CLSM data and calculated as the particle-to-particle variation, and dR/dpH is the gradient in the R versus pH plot. The standard deviation σ_{pH} reflects the particle-to-particle variation in R measured at a given pH. The value of σ_{pH} is smaller than 0.8 at pH 7 and rapidly decreases with decreasing pH until pH 5.5, where $\sigma_{pH} < 0.2$. The M270-SNARF particles are most sensitive between pH 5 and 6. It is important to note that measurement of pH changes determined using the fluorescence ratio R obtained for a single particle is achieved with a much higher accuracy of 0.03, calculated as the standard deviation of a time series of pH measurements using a sin-

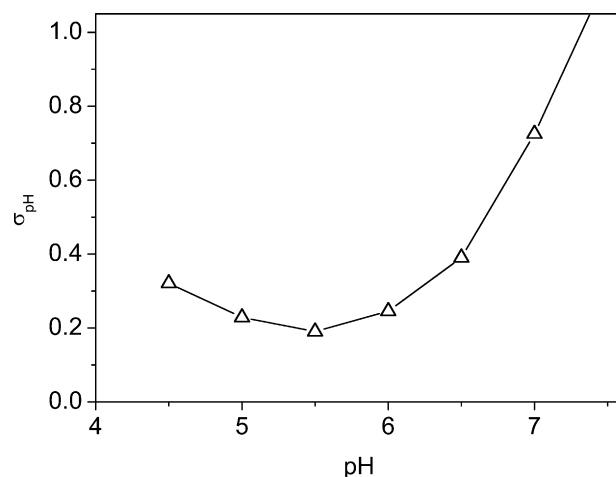


Fig. 5. Standard deviation σ_{pH} as a function of pH for the M270-SNARF particles.

gle M270-SNARF particle at pH 7 (data not shown). This means that the accuracy achieved when measuring changes in pH (e.g. inside a phagosome during phagocytosis of a single particle) as a function of time is more than an order of magnitude higher than the accuracy achieved in absolute measurements of pH.

For live cell experiments, RAW 264.7 macrophages were allowed to internalize M270-SNARF particles. The subsequent phagosome acidification was monitored in real-time using CLSM.

Fig. 6a shows a set of time-lapse images (CLSM images of channels 1 and 2 overlaid on white light transmission image) of an M270-SNARF particle being phagocytosed by a macrophage (See [Supplementary Information](#) for the full movie). In these images the (false) color of the M270-SNARF particle is a measure of local pH. The particle color slowly changes to green, i.e. a decrease in signal in channel 2 and an increase in channel 1, demonstrating the acidification of the particles (lower pH). During this time,

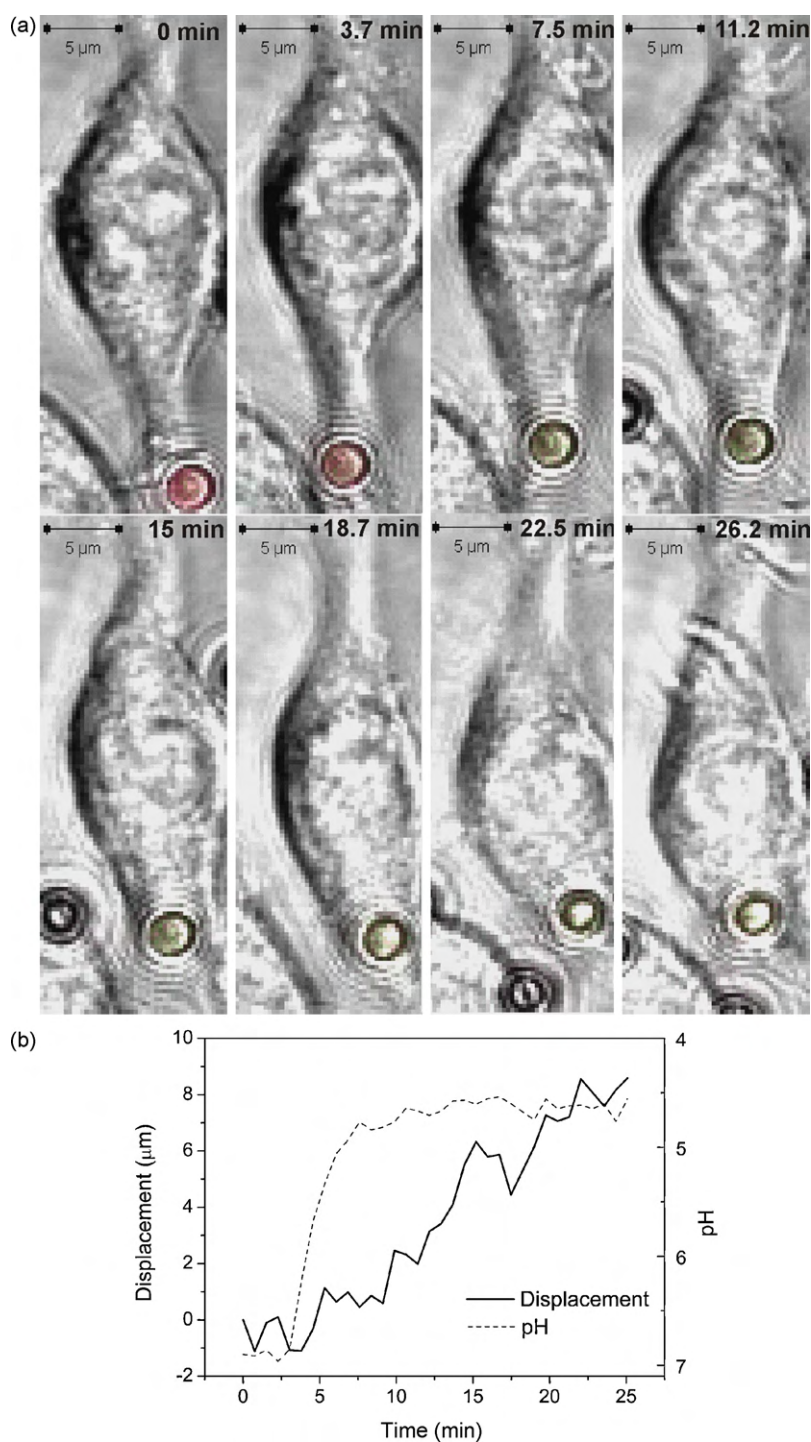


Fig. 6. (a) Time-lapse CLSM images of a M270-SNARF particle being phagocytosed by a RAW 264.7 macrophage. The elapsed time between each image is 225 s. The images shown are an overlap of white light transmission image, CLSM image taken at channels 1 (false color green) and channel 2 (false color pink). The resulting color is indicative for the ratio R which in turn is a measure of the pH of the phagosome. The observed color change from pink at the first frame to green in the last frame indicates a pH drop from approximately 6.8 to 5.0. The scale bar corresponds to 5 μm. (See [Supplementary Data](#) for full movie). (b) The figure shows a plot of displacement and pH of the particle as a function of time. (For interpretation of the references to color in this figure legend, the reader is referred to the web version of the article.)

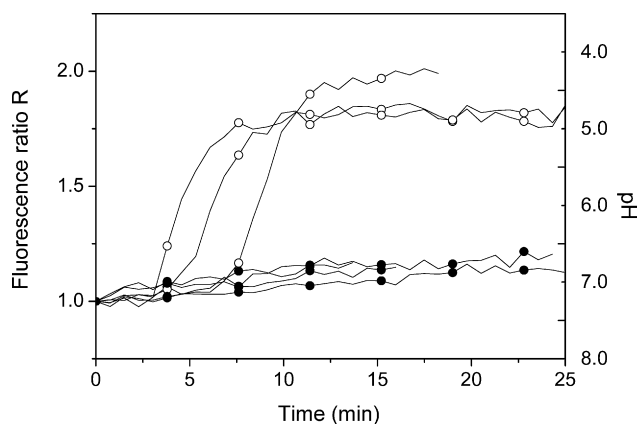


Fig. 7. Fluorescence ratio of phagocytosed (open symbols) and non-phagocytosed (solid symbols) M270-SNARF particles over time. Each curve represents the data obtained for a single particle. Similar results were obtained for multiple experiments and only a representative subset of the data has been shown here.

the particle is also seen to move towards the cell nucleus. Fig. 6b shows a plot of displacement (with respect to the nucleus) and pH of the particle as a function of time. From the figure it is seen that the particle continues to move even after the acidification has stopped. Particles that were not taken up by macrophages did not show any significant change in fluorescence over time.

Fig. 7 shows some examples of the changes in fluorescent intensity ratio R of M270-SNARF particles as a function of time during phagocytosis of these particles by RAW 264.7 macrophages. For comparison, traces of particles that are not phagocytosed during the experiment are also displayed. The fluorescence ratios R are normalized such that at the beginning of the experiment the ratio $R=1$. The pH of the cell culture medium was determined to be 6.8. During the assay, some particles are engulfed by macrophages and are acidified as indicated by the increase in the ratio from $R=1$ to $R \approx 2$. The increase in fluorescence ratio corresponds to a decrease in pH from pH 6.8 to ≈ 4.5 . The acidification of the phagosome takes around 5 min, after which the compartmental pH stabilizes. The particles which remain outside the macrophages all show a small increase in the fluorescence ratio which may be most likely attributed to a small drift in the medium pH or to differential photo-bleaching between Snarf-4f and the autofluorescence of the particles. Measurement of the change in pH using M270-SNARF particles has been carried out on at least 25 different cells. They all show similar time-dependent reduction in pH. However, the movement of the particle towards the nucleus varied depending upon the position on the plasma membrane where the particle gets internalized.

Next, an external magnetic force was applied on the M270-SNARF particle allowing the manipulation of the sensor inside the cell while simultaneously measuring the local pH. Fig. 8a shows an example of an M270-SNARF particle that is phagocytosed by a RAW 264.7 macrophage and then moved actively through the cell by the magnetic tweezers. The pH change inside the phagosome containing the M270-SNARF particle is monitored simultaneously. In this example the MT is placed within a distance of $100 \mu\text{m}$ from the cell and the applied force is $\sim 100 \text{ pN}$. The average velocity of the particle during manipulation was measured to be 25 nm/s . In Fig. 8b the displacement of the M270-SNARF particle and the measured pH as a function of time is plotted for the example given in Fig. 8a. Fig. 8b also shows the position of the particle with respect to the cell. Clearly when the particle/phagosome reaches the cell periphery, the movement is limited by the elasticity of the cell membrane. However, the amplitude of the force is such that the membrane

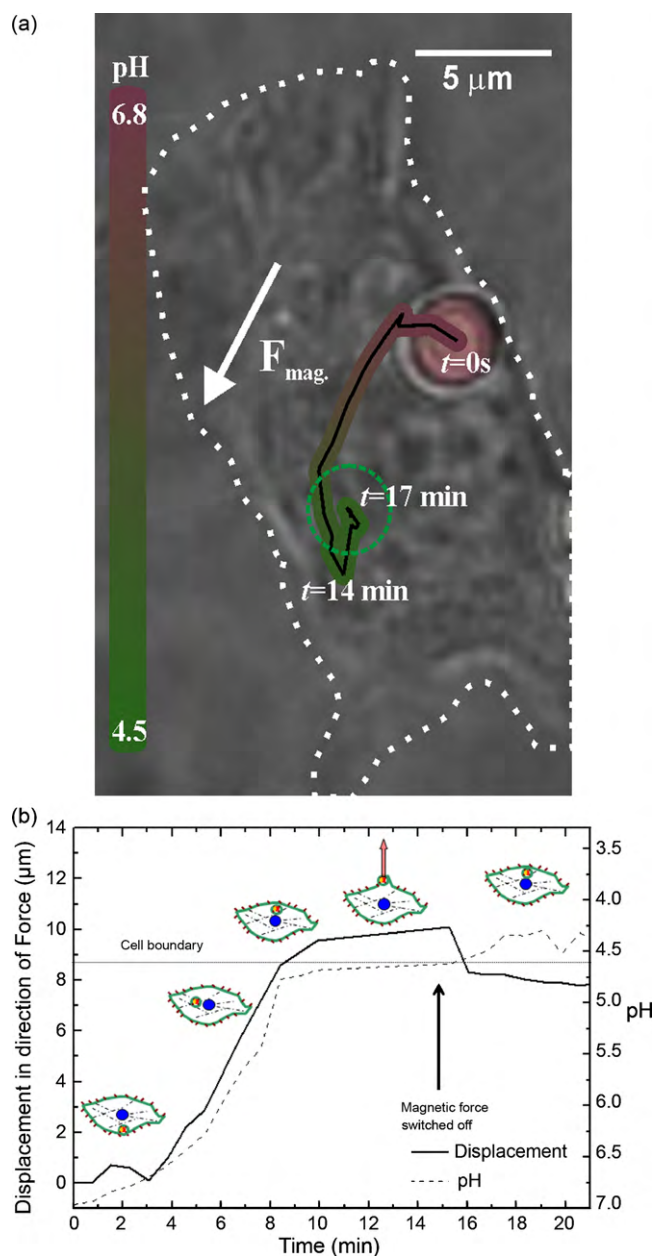


Fig. 8. (a) White light transmission microscopy image of a pH-sensing magnetic particle phagocytosed by a RAW 264.7 macrophage, with an overlay of the particle trajectory which is color-coded for pH of the phagosome. The white arrow indicates the direction of the applied force (100 pN) on the magnetic particle by the MT. The green circle indicates the final position of the particle. At $t=0 \text{ s}$, the MT is switched on, at $t=14 \text{ min}$, the MT is switched off. The dotted white line denotes the cell boundary. The scale bar corresponds to $5 \mu\text{m}$ (See Supplementary Data for the full movie). (b) Position (solid line) and pH (dashed line) of the magnetic particle (shown in Fig. 8a) under the application of a magnetic force plotted against time. Insets in the figure schematically show the position of the bead relative to the cell and the direction of the applied force at different time-points in the experiment. When the particle reaches the periphery of the cell (indicated by the horizontal dotted line) the elasticity of the membrane prevents further displacement of the particle. After switching off the magnetic tweezers (indicated by the black arrow), the particle is pushed back by the elastic membrane. (For interpretation of the references to color in this figure legend, the reader is referred to the web version of the article.)

deforms. After 14 min, when the MT is switched off, the particle moves inwards as a result of the elasticity of the cell membrane. Interestingly the pH appears to further decrease after the particle is pushed more inside the cell by the elastic forces of the membrane. This suggests that by active repositioning of the phagosome it is possible to influence the maturation of the phagosome. Similar

behaviour has been observed in 4 out of 20 phagosomes that were spatially manipulated.

4. Discussion

We have shown that it is possible to measure a local intracellular chemical property in a spatially resolved manner while simultaneously remotely moving the magnetic particle inside a cell. We have developed a chemical sensor that can be spatially controlled by functionalizing magnetic particles with a fluorescent dye sensitive to a particular chemical species. The fluorescent dye allows the measurement of the chemical property and the magnetic content of the particle allows for the intracellular manipulation, thereby together allowing local and spatially resolved chemical sensing.

One of the problems encountered in the fabrication of chemical sensing magnetic particles is that the magnetic content of the particle may limit the sensing properties of the dye. For instance, Anker et al. reported the loss of all pH-sensing capabilities of Snarf-1 when coupled to high magnetic content particles [18]. Furthermore, the fluorescence intensity may be quenched on the surface of a magnetic core by non-radiative energy transfer or by the strong absorption of the transmitted light by the core [25]. Also, Liu et al. showed a large red shift and peak narrowing in the fluorescence intensity of fluorescein when coupled to magnetic nanospheres [26]. In our experiments, the match between the measured fluorescence ratios with those reported in literature suggests that the pH-dependent fluorescence of Snarf-4f was not influenced by the coupling of the dye to the magnetic particle [27].

The accuracy of pH measurements of M270-SNARF is typically within ~ 0.3 pH units, whereas the accuracy to measure pH changes with a single particle is ~ 0.03 pH units. This accuracy is in the same order of magnitude as that typically found for Fluorescein coupled to non-magnetic polymer or silica particles. For instance, McNamara et al. [28] and Peng et al. [29] reported accuracies of 0.1 and 0.05, respectively. However, these are derived from fluorescence spectroscopy measurements on bulk samples. The accuracy may be further improved by reducing the autofluorescence of the Dynabeads.

Since the accuracy in measuring pH changes using a single particle is an order of magnitude larger than the absolute pH measurements, the use of a single particle that can be maneuvered to different positions within the cell may yield more accurate data than the use of multiple particles randomly distributed inside the cell. This observation illustrates one of the advantages of the approach developed here compared to those that use non-magnetic sensor particles.

During the process of phagocytosis the particle remains enclosed in a membrane. However, the sensing particles can easily be introduced directly into the cytoplasm, nucleus or other organelles using available techniques like micro/pico-injection, gene-gun delivery, liposome incorporation, nonspecific or receptor-mediated endocytosis with surface-conjugated translocating proteins/peptides, and membrane-penetrating TAT peptides used by human immunodeficiency virus [5].

The particles used in this work are relatively large; however we have earlier shown that it is possible to magnetically manipulate much smaller (350 nm) magnetic particles inside a living cell [16]. It should therefore be straightforward to develop magnetic particle-based chemical sensors using particles of various sizes depending upon the specific application.

Although here we have used pH as a measurable property, the principle of using magnetic particles for chemical sensing, as is demonstrated here, is not limited to measuring pH in phagosomes alone but can also be applied to sense other analytes. For example, a Ca^{2+} sensing fluorescent dye can be attached to the magnetic

particle and the particle can be moved through the cell (both in the cytoplasm and inside organelles) to measure local calcium concentrations. Moreover, multiple dyes sensing different analytes can, in principle, be attached to the same magnetic particle thus permitting simultaneous measurement of multiple chemical species provided there is no significant overlap between the spectra of the dyes.

Besides the measurement of chemical properties at different sites within the cell, the approach developed here also shows other promising applications in the field of cell biophysics. One interesting concept is to use the application of force, or the movement of organelles to interfere with the normal functioning of the cell. Simultaneously the response of the cell can be monitored. One possibility is to study the relationship between maturation of the phagosome and its intracellular position. Phagocytosis involves the transport of the particle-containing compartment (phagosome) from the plasma membrane to the cell nucleus. During this normal movement of the phagosome towards the nucleus, the phagosome fuses with lysosomes which leads to the acidification of the compartment. Currently it is unknown, how important the position of the phagosome is in relation to acidification. The magnetic nature of our sensor permits us to alter the movement of the phagosome towards the nucleus, i.e. retard the movement and keep the particle at the plasma membrane or accelerate the particle's movement to the nucleus. In the future this system could also be used to study the effect of accelerating or retarding the movement on the rate of acidification. Additionally these particles could also be used for studying the chemical response of a cell to mechanical stimulation or vice-versa, for example with muscle cells that react mechanically to a change in local chemical concentration.

5. Conclusions

We have successfully developed a new approach that allows spatially resolved local intracellular chemical sensing using a hybrid magnetic chemical sensor which can be actively manipulated using magnetic tweezers. As a proof-of-principle we have moved a pH-sensing magnetic particle inside a living cell while simultaneously measuring the local pH. In addition it appears to be possible to actively interfere with the cell function by manipulating cell organelles with the magnetic tweezers. Finally, we believe that this method is a promising new tool to study intracellular processes.

Acknowledgments

We acknowledge funding from the Framework Programme of the European Commission, Fluoromag (contract number 037465-FLUOROMAG) and Immunomop (contract number MRTN-CT-2006-035946).

Appendix A. Supplementary data

Supplementary data associated with this article can be found, in the online version, at [doi:10.1016/j.snb.2010.05.006](https://doi.org/10.1016/j.snb.2010.05.006).

References

- [1] M.E. Greenberg, M.A. Thompson, M. Sheng, Calcium regulation of immediate early gene-transcription, *Journal of Physiology-Paris* 86 (1992) 99–108.
- [2] E. Carafoli, Calcium signaling: a tale for all seasons, *Proceedings of the National Academy of Sciences of the United States of America* 99 (2002) 1115–1122.
- [3] I. Heilmann, M.S. Pidkowich, T. Girke, J. Shanklin, Switching desaturase enzyme specificity by alternate subcellular targeting, *Proceedings of the National Academy of Sciences of the United States of America* 101 (2004) 10266–10271.
- [4] B.P. Tu, A. Kudlicki, M. Rowicka, S.L. McKnight, Logic of the yeast metabolic cycle: temporal compartmentalization of cellular processes, *Science* 310 (2005) 1152–1158.

- [5] Y.E.K. Lee, R. Smith, R. Kopelman, Nanoparticle PEBBLE sensors in live cells and in vivo, *Annual Review of Analytical Chemistry* 2 (2009) 57–76.
- [6] S.M. Buck, H. Xu, M. Brasuel, M.A. Philbert, R. Kopelman, Nanoscale probes encapsulated by biologically localized embedding (PEBBLEs) for ion sensing and imaging in live cells, *Talanta* 63 (2004) 41–59.
- [7] H. Sun, A.M. Scharff-Poulsen, H. Gu, I. Jakobsen, J.M. Kossmann, W.B. Frommer, K. Almdal, Phosphate sensing by fluorescent reporter proteins embedded in polyacrylamide nanoparticles, *ACS Nano* 2 (2008) 19–24.
- [8] T.C. O'Riordan, K. Fitzgerald, G.V. Ponomarev, J. Mackrill, J. Hynes, C. Taylor, D.B. Papkovsky, Sensing intracellular oxygen using near-infrared phosphorescent probes and live-cell fluorescence imaging, *American Journal of Physiology-Regulatory Integrative and Comparative Physiology* 292 (2007) R1613–R1620.
- [9] Y.F. Cao, Y.E.L. Koo, S.M. Koo, R. Kopelman, Ratiometric singlet oxygen nanoprobes and their use for monitoring photodynamic therapy nanoplatforms, *Photochemistry and Photobiology* 81 (2005) 1489–1498.
- [10] M. King, R. Kopelman, Development of a hydroxyl radical ratiometric nanoprobe, *Sensors and Actuators B: Chemical* 90 (2003) 76–81.
- [11] S.H. Kim, B. Kim, V.K. Yadavalli, M.V. Pishko, Encapsulation of enzymes within polymer spheres to create optical nanosensors for oxidative stress, *Analytical Chemistry* 77 (2005) 6828–6833.
- [12] H. Xu, J.W. Aylott, R. Kopelman, Fluorescent nano-PEBBLE sensors designed for intracellular glucose imaging, *Analyst* 127 (2002) 1471–1477.
- [13] A. Myc, I.J. Majoros, T.P. Thomas, J.R. Baker Jr., Dendrimer-based targeted delivery of an apoptotic sensor in cancer cells, *Biomacromolecules* 8 (2007) 13–18.
- [14] N. Baker, G.M. Greenway, R.A. Wheatley, C. Wiles, A chemiluminescence nanosensor to monitor lipid peroxidation, *Analyst* 132 (2007) 104–106.
- [15] A.H. de Vries, B.E. Krenn, R. van Driel, J.S. Kanger, Micro magnetic tweezers for nanomanipulation inside live cells, *Biophysical Journal* 88 (2005) 2137–2144.
- [16] A.H.B. de Vries, B.E. Krenn, R. van Driel, V. Subramaniam, J.S. Kanger, Direct observation of nanomechanical properties of chromatin in living cells, *Nano Letters* 7 (2007) 1424–1427.
- [17] T.G. Roberts, J.N. Anker, R. Kopelman, Magnetically modulated optical nanoprobe (MagMOONs) for detection and measurement of biologically important ions against the natural background fluorescence of intracellular environments, *Journal of Magnetism and Magnetic Materials* 293 (2005) 715–724.
- [18] J.N. Anker, Y.E. Koo, R. Kopelman, Magnetically controlled sensor swarms, *Sensors and Actuators B: Chemical* 121 (2007) 83–92.
- [19] R.M.C. Dawson, D.C. Elliot, W.H. Elliot, K.M. Jones, *Data for Biochemical Research*, Oxford Science Publ., 1986.
- [20] J. Ji, N. Rosenzweig, C. Griffin, Z. Rosenzweig, Synthesis and application of sub-micrometer fluorescence sensing particles for lysosomal pH measurements in murine macrophages, *Analytical Chemistry* 72 (2000) 3497–3503.
- [21] J.A. Champion, S. Mitragotri, Role of target geometry in phagocytosis, *Proceedings of the National Academy of Sciences of the United States of America* 103 (2006) 4930–4934.
- [22] S.E.A. Gratton, P.A. Ropp, P.D. Pohlhaus, J.C. Luft, V.J. Madden, M.E. Napier, J.M. DeSimone, The effect of particle design on cellular internalization pathways, *Proceedings of the National Academy of Sciences of the United States of America* 105 (2008) 11613–11618.
- [23] N. Marcotte, A.M. Brouwer, Carboxy SNARE-4F as a fluorescent pH probe for ensemble and fluorescence correlation spectroscopies, *Journal of Physical Chemistry B* 109 (2005) 11819–11828.
- [24] M. Salerno, J.J. Ajimo, J.A. Dudley, K. Binzel, P. Urayama, Characterization of dual-wavelength seminaphthofluorescein and seminaphthorhodafuor dyes for pH sensing under high hydrostatic pressures, *Analytical Biochemistry* 362 (2007) 258–267.
- [25] S.A. Corr, Y.P. Rakovich, Y.K. Gun'ko, Multifunctional magnetic-fluorescent nanocomposites for biomedical applications, *Nanoscale Research Letters* 3 (2008) 87–104.
- [26] H.B. Liu, J. Guo, L. Jin, W.L. Yang, C.C. Wang, Fabrication and functionalization of dendritic poly(amidoamine)-immobilized magnetic polymer composite microspheres, *Journal of Physical Chemistry B* 112 (2008) 3315–3321.
- [27] M. Valli, M. Sauer, P. Branduardi, N. Borth, D. Porro, D. Mattanovich, Intracellular pH distribution in *Saccharomyces cerevisiae* cell populations, analyzed by flow cytometry, *Applied and Environmental Microbiology* 71 (2005) 1515–1521.
- [28] K.P. McNamara, T. Nguyen, G. Dumitrascu, J. Ji, N. Rosenzweig, Z. Rosenzweig, Synthesis, characterization, and application of fluorescence sensing lipobeads for intracellular pH measurements, *Analytical Chemistry* 73 (2001) 3240–3246.
- [29] J.F. Peng, X.X. He, K.M. Wang, W.H. Tan, Y. Wang, Y. Liu, Noninvasive monitoring of intracellular pH change induced by drug stimulation using silica nanoparticle sensors, *Analytical and Bioanalytical Chemistry* 388 (2007) 645–654.

Biographies

Shashank Shekhar (1985) received his B.Sc. in physics at Loyola College (2005, University of Madras, India). He was then awarded an Erasmus Mundus Masters fellowship to carry out a double M.Sc. in Nanoscience (2007, University of Leiden and Technical University of Delft, Netherlands) and Molecular Bioengineering (2007, Technical University of Dresden, Germany). In October 2007, he started his Ph.D. as a Marie Curie fellow as part of the European Consortium IMMUNANOMAP at the Nanobiophysics group at the University of Twente, The Netherlands, where he has since been working.

Arjen Klaver received his M.Sc. degree in applied physics from Eindhoven University of Technology in 2001. He then earned his Ph.D. at DIMES, Delft University of Technology, The Netherlands in 2007. From 2007 to 2009, he worked as a post-doctoral researcher at the Nanobiophysics group at the University of Twente, The Netherlands in the area of biological applications of magnetic tweezers as part of the European Consortium FLUOROMAG.

Carl Figdor graduated from University of Utrecht in The Netherlands (1979). He then received his Ph.D. at the Netherlands Cancer Institute (1982, University of Amsterdam). In 1992 he became a professor in cell biophysics at University of Twente. In 1994, he moved to the Radboud University Nijmegen as a professor in Immunology where he initiated research on molecular mechanisms of dendritic cells and their role as antigen presenting cells. Since 2001, he has been the scientific director of Nijmegen Centre for Molecular life Sciences. In 2006 he was awarded the Spinoza premium for his scientific contributions. In 2008 he was awarded member of the royal Netherlands academy of arts and sciences.

Vinod Subramaniam received his B.Sc. in electrical engineering from Cornell University in 1989. He then earned a M.Sc. in applied physics and a M.Sc. in engineering in electrical engineering in 1992 and a Ph.D. in applied physics in 1996 from the University of Michigan, Ann Arbor. He is currently professor at the University of Twente, leading the Nanobiophysics group. Professor Subramaniam's current research interests are in molecular and cellular biophysics, focusing on protein misfolding and aggregation, and nanobiophotonics.

Johannes S. Kanger (1968) received the M.Sc. degree (1992) in applied physics and the Ph.D. degree (1996) from the University of Twente, Enschede, The Netherlands. From 1996 to 1998, he worked as a postdoctoral fellow in the field of biomedical optics and noninvasive diagnostics. Since 1999, he has been working in the nanobiophysics group at the University of Twente as a senior scientist in cell biophysics and advanced microscopy. His main interests are magnetic tweezers, optical tweezers, cell biophysics, and optical biosensors.